Available online at www.sciencedirect.com
ScienceDirect
Remote Sensing of Environment 108 (2007) 240–253
Remote Sensing of Environment
www.elsevier.com/locate/rse

Observations of Lake Baikal ice from satellite altimetry and radiometry

Alexei V. Kouraev [a,b,*], Sergei V. Semovski [c,✠], Michail N. Shimaraev [c], Nelly M. Mognard [a], Benoît Légresy [a], Frédérique Remy [a]

[a] *Laboratoire d'Etudes en Géophysique et Océanographie Spatiales (LEGOS), Toulouse, France*
[b] *State Oceanography Institute, St. Petersburg branch, Russia*
[c] *Limnological Institute, Siberian Branch of Russian Academy of Sciences, Irkutsk, Russia*

Received 5 January 2006; received in revised form 9 November 2006; accepted 11 November 2006

Abstract

We demonstrate the potential of combining satellite altimetry and radiometry for lake ice studies using the example of Lake Baikal in Siberia. We show the synergy using active and passive microwave observations available from the recent satellite altimetry missions (TOPEX/Poseidon, Jason-1, ENVISAT and Geosat Follow-On), complemented by the SSM/I passive data. We assess the applicability of altimetric and radiometric data for ice/water discrimination, and discuss the drawbacks and benefits of each type of sensor. An ice discrimination method, based on the combined use of the data from the four altimetric missions and SSM/I, is proposed and validated using available in situ observations and MODIS imagery. The method is applied to the entire satellite data set and used to define specific dates of ice events (first appearance of ice, formation of stable ice cover, first appearance of open water, complete disappearance of ice) and associated uncertainties. Using these satellite-derived estimates, we can extend the existing time series of ice events in the Southern Baikal up to 2004 and provide new information on the Middle and Northern Baikal, regions where no recent in situ ice cover observations are available. Our data show that over the last 10–15 years, trends towards earlier ice formation and later ice break-up result in a tendency for longer fast ice duration over the whole Lake Baikal. The methods proposed here have been tested for Lake Baikal, but they are applicable for other lakes and water bodies with seasonal ice cover.

Keywords: Lake Baikal; Lake ice; Satellite altimetry and radiometry; Combination of active and passive microwave data

1. Introduction

Lake Baikal, a UNESCO World Heritage site, is the deepest lake in the world and represents 20% of the world's unfrozen freshwater resources. The lake's unique natural conditions and rich flora and fauna attract many researchers who study its ecosystem dynamics and its susceptibility to climate change and human perturbation.

More than 300 rivers flow into the Lake Baikal, bringing about 60 km^3 of water per year (Galaziy, 1987). Selenga is the largest, supplying about half of the total river input from its watershed of 465,000 km^2. Other main rivers include the Barguzin and the Verhnyaya Angara (Fig. 1). The Angara river regulates the lake level since it is the only river that flows out of Lake Baikal.

Bathymetric features separate the lake into three distinct basins (see Fig. 1). The southern basin (maximal depth 1461 m) (INTAS Project 99-1669, 2002) is separated by the shallow Selenga sill (maximal depth 360 m). The middle basin is the deepest (maximal depth 1642 m) and is bounded to the north by the Akademicheskiy ridge (maximal depth 260 m). The northern basin is relatively shallow (depths less than 900 m). Morphological features define the particularities of the water dynamics and other natural conditions for each of the Lake Baikal parts, and they are often referred to as the Southern, Middle and Northern Baikal.

Lake Baikal is located in the central Asian continent, where climate conditions are strongly continental, with a mean annual

* Corresponding author. Laboratoire d'Etudes en Géophysique et Océanographie Spatiales (LEGOS), 18 Avenue Edouard Belin, 31401, Toulouse Cedex 9, France. Tel.: +33 561 33 29 37.
E-mail addresses: kouraev@notos.cst.cnes.fr (A.V. Kouraev), shimarae@lin.irk.ru (M.N. Shimaraev), nelly.mognard@cnes.fr (N.M. Mognard), Benoit.Legresy@legos.obs-mip.fr (B. Légresy), frederique.remy@legos.obs-mip.fr (F. Remy).
✠ Sergei V. Semovski sadly passed away on 2nd June 2006.

0034-4257/$ - see front matter © 2006 Elsevier Inc. All rights reserved.
doi:10.1016/j.rse.2006.11.010

Fig. 1. General map of the Lake Baikal region. Black dots locate the maximal depth in the three parts of the lake. A—Selenga sill, B—Akademicheskiy ridge.

temperature of −1.3 °C in the south and −3.2 °C in the north. Long, cold winters result in the complete freeze-up of the lake every year for 5–6 months. According to historical data (Atlas of the Lake Baikal, 1993; Verbolov et al., 1965) ice formation starts in late December–early January in the Northern Baikal and in the first half of January in the Southern Baikal. Ice break-up starts in early-May in the Southern part of the lake, and in mid-May in the north.

The state of the lake ice cover and snow its overlying determine the formation of different hydrophysical fields and influence spring the bloom of diatoms and primary productivity (Granin et al., 1999; Mackay et al., 2003, 2005; Semovski et al., 2000). During late winter and early spring when the lake is still ice-covered, intense development of phytoplankton, zooplankton and benthos starts under the ice, due to the high transparency of the Baikal ice. The algal bloom intensity depends on the optical properties of ice, and the term dynamics of the primary production is thus associated with changes in the freeze-up duration.

Ice and snow conditions influence the living conditions of the only Baikal mammal – the Baikal seal (*Phoca sibirica*). The seals give birth to their offspring in the snow caves on the ice from the end of February to the beginning of April. During winters with thin snow cover it is difficult for the seals to construct these snow caves. As a result, many baby seals die, and the number of crows which feed on them rapidly increases.

The ice cover is also important for ice transport, for fishing activities and tourism. During winter the ice is strong enough to support roads, and the narrow lake width allows transport to rapidly reach the opposite coast.

Lake Baikal's ice cover and other natural conditions have been studied extensively for more than a century (Atlas of the Lake Baikal, 1993; Shimaraev et al., 2002b; Verbolov et al., 1965; Wüest et al., 2005). The state of the ice cover, and the dynamics of the freezing and break-up cycles are good indicators of large-scale climate changes. The existing data have been used for various climatic studies, relating ice conditions in the southern Baikal with global climatic variability (Livingstone, 1999; Magnuson et al., 2000; Shimaraev et al., 2003; Todd & Mackay 2003). Most of the published articles are based on the longest homogeneous time series of dates of ice formation and break up available from the Listvyanka coastal station (see Section 2.2.1).

Observations at coastal stations are very valuable, but many parts of the lake remain relatively unexplored. The lake dimensions are enormous and its natural climate conditions are inhomogeneous. Different parts of the lake have specific systems of atmospheric circulation and precipitation. For example, the climate in the northern part is more severe, influenced by the Yakut anticyclone (Siberian High) (Semovski & Mogilev, 2003). These particularities in natural climate conditions stress the necessity of lake-wide ice monitoring.

Such monitoring has been done on a regular basis using aerial surveys and field expeditions. Until 1982, a total of 120 schematic maps were generated for the ice conditions of certain parts of the lake's surface. However, due to financial constraints, the number of observations has sharply decreased since the mid-1980s.

The lack of in situ information was compensated later by the use of satellite imagery, mainly in the visible and infrared range (especially from low-resolution Soviet weather satellites "Meteor"). More recently, Baikal ice monitoring has been performed using visible range sensors such as AVHRR (Advanced Very High Resolution Radiometer) onboard NOAA (National Oceanic and Atmospheric Administration) polar-orbiting satellites and MODIS (Moderate Resolution Imaging Spectroradiometer) onboard the Terra and Aqua satellites, as well as some limited ERS SAR (Synthetic Aperture Radar) images (Semovski & Mogilev, 2003; Semovski et al., 2000). Since December 2002, a satellite receiving station in Irkutsk is obtaining optical imagery from the MODIS sensor (Irkutsk RICC website, 2000).

However, satellite data in the visible and infrared range can be sporadic due to the presence of cloud cover and fog. Clouds over Lake Baikal are relatively rare compared to the neighbouring mountainous regions, since the air masses lose their water vapour on the external slopes and air subsiding over the lake is relatively dry. However, cloudy periods are often observed. More problematic is the presence of fog, especially in late autumn and early winter, when cold air masses come over the warmer lake surface, forming a thin (about 1 m thick) layer of fog. During this time evaporation from the lake surface is 2–3 times larger than in the summer (Galaziy, 1987).

The use of microwave satellite observations represents a step forward, providing reliable, regular and weather-independent data on ice cover. For more than two decades the scientific community has used passive microwave data from the SMMR (Scanning Multichannel Microwave Radiometer) and the SSM/I (Special Sensor Microwave/Imager) instruments to estimate ice cover extent and type both in the Arctic and in the Antarctic. Passive radiometric data have also been successfully combined with optical and infrared observations from other satellites (Emery

et al., 1994). During the 1984 Marginal Ice Zone Experiment (MIZEX) ice cover has been studied using simultaneous observations from passive (radiometers) and active (SAR) sensors during aircraft flights (Burns et al., 1987; Cavalieri et al., 1990). Studies of sea ice using simultaneous active and passive observations from the same satellite platform have been made using OKEAN-01 radiometer RM-08 and side-looking radar RLS-BO data from 1995 to 1997, and an ice concentration algorithm using a linear mixture model has been proposed (Belchansky & Douglas, 2000, 2002).

In this paper we explore how freshwater lake ice studies (on the example of Lake Baikal) can benefit from the synergy of using passive and active microwave satellite data from another type of satellite sensors: e.g. the long time series of simultaneous nadir-looking active and passive observations available from the four recent satellite altimetry missions (TOPEX/Poseidon, Jason-1, ENVISAT and Geosat Follow-On). In order to increase spatial resolution, we complement these observations by passive data from SSM/I sensor. The goals of this paper are:

1) to assess the applicability of altimetric and radiometric data for lake ice/ open water discrimination, and discuss the drawbacks and benefits of each type of sensor;
2) to propose a lake ice discrimination approach based on a combined use of the data from the four altimetric missions and SSM/I;
3) to validate and apply the ice/water discrimination method to Lake Baikal using the available satellite data for 1992–2004;
4) to extend the existing time-series of ice cover formation and break-up dates for the Southern Baikal and provide new time series for the Middle and Northern Baikal;
5) to compare the resulting satellite-derived time series of dates of ice cover formation and break-up dates in the with existing observations at coastal stations and other satellite and in situ data.

2. Data

2.1. Microwave satellite data

2.1.1. Satellite altimetry

We have used data from several radar altimetry missions (Table 1, Fig. 2). The earliest data are available from the TOPEX/Poseidon (T/P) satellite, operating since 1992 and

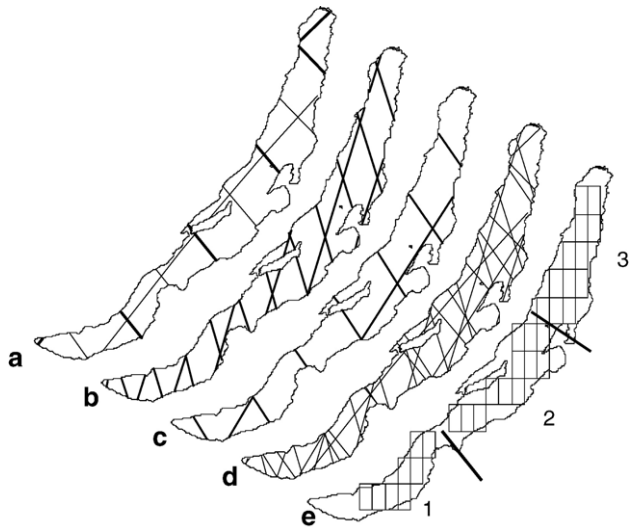

Fig. 2. Satellite ground track coverage of Lake Baikal. (a) T/P and Jason-1 (bold lines) and T/P new orbit (thin lines); (b) ENVISAT; (c) GFO; (d) all (a+b+c) altimetric ground tracks, (e) selected EASE-grid pixels of SSMI observations (rectangles) and three sub-regions of Baikal: 1—Southern, 2—Middle, 3—Northern Baikal.

followed by Jason-1, orbiting on the same ground track since February 2002. In August 2002, T/P was maneuvered onto a new orbit (referred as TPNO), flying halfway between its previous tracks. This new orbit provides interesting data for our study as one of its ascending ground tracks crosses the whole lake. The T/P mission ended in October 2005. The T/P, TPNO and Jason-1 data are complemented by observations from recent radar altimeters onboard Geosat Follow-On (GFO) (since January 2000) and ENVISAT (since November 2002) satellites.

All four altimeters have two main nadir-looking instruments—a dual-frequency (single-frequency for GFO) radar altimeter operating in Ku (13.6 GHz), C (5 GHz) or S (2 GHz) bands, and a passive microwave radiometer operating at two or three frequencies (see Table 1). These sensors have various footprint size. For example, for the T/P radar altimeter, the footprint diameter in Ku-band is between 10 and 12 km (depending on the surface roughness), while for its radiometers operating at 18, 23, and 37 GHz the footprint diameter is 42, 35, and 22 km, respectively. The fact that these are simultaneous observations from the same platform significantly enhances the data analysis capability. The repeat period ranges from 10 days for T/P and Jason-1 to 35 days for ENVISAT. We use 1 Hz data which provide

Table 1
Main parameters of satellite altimetry and radiometry missions and data used in this study (frequencies used are in bold)

Satellite	Radar altimeter, band[a]	Radiometer frequencies, GHz	Cycles used	Time	Repeat cycle, days
TOPEX/Poseidon (T/P)	C, **Ku**	**18**, 21, **37**	1–365	September 1992–August 2002	10
T/P new orbit (TPNO)	C, **Ku**	**18**, 21, **37**	368–437	September 2002–September 2004	10
Jason-1	C, **Ku**	**18**, 21, **37**	79–214	February 2002–October 2004	10
ENVISAT	**Ku** and S	**18.7**, 23.8, **34**	11–30	November 2002–November 2004	35
Geosat Follow-On (GFO)	**Ku**	**22**, **37**	37–143	January 2000–January 2005	17
SSM/I	no	**19.35 (H,V)**, 22.235, **37.0 (H,V)**, 85.5 (H,V)		January 1992–October 2003	5

[a] Ku band—13.6 GHz, C band—5 GHz, S band—2 GHz.

an along track ground resolution of about 6 km. The altimetry data were obtained from the Centre for Topographic studies of the Oceans and Hydrosphere (CTOH) at the LEGOS laboratory.

2.1.2. Passive microwave data

The passive microwave data from SSM/I (Special Sensor Microwave/Imager) on board the DMSP (Defence Meteorological Satellite Program) series are available since 1987. The SSM/I radiometers, with incidence angle ranging from 50.2 to 52.8 degrees, provide measurements of brightness temperature at different frequencies and at different (vertical or horizontal) polarisation (see Table 1). The National Snow and Ice Data Center (NSIDC) provided the SMMR and SSMI data mapped onto an Equal-Area Scalable Earth Grid (EASE-Grid) projection with 625 km^2 spatial resolution (Armstrong et al., 2003). The initial data were averaged to obtain pentad (5-day) mean values to provide continuous spatial coverage. We have used SSM/I data starting from 1992 (the beginning of the T/P mission).

2.1.3. Geographical selection

We performed a geographical selection of the data in order to minimise the potential contamination of the T/P and SSM/I signal by land reflections, and to retain a sufficiently large number of altimeter and radiometer measurements over water. For the altimetry data, we have excluded data closer than 1 km from the coast, and for the SSM/I data we have excluded EASE-grid pixels when more than 30% of the pixel covers coastal regions or islands. We have further divided the data set into three sub-regions: Southern, Middle and Northern Baikal (see Fig. 2). Each sub-region has good SSM/I and satellite altimetry coverage (see also Section 3.1). We have also identified two smaller sub-regions in the vicinity of stations Listvyanka (the two EASE-grid pixels in the extreme south-west) and Nizhneangarsk (two most northern pixels) for comparison with the in situ observations at these stations.

2.2. Ancillary data

2.2.1. Observations at coastal stations and corrections of the NSIDC database

Baikal's ice conditions have been studied using coastal station measurements since 1869. In our work we have used the ice phenology observations from the Limnological Institute of the Russian Academy of Sciences (LIN RAS) from the Listvyanka station. Long time-series of ice formation, break up dates and ice duration observed at coastal stations are also available at the Lake and River Ice Phenology Database at NSIDC (National Snow and Ice Data Center) (Benson & Magnuson, 2000). However, we have found several inconsistencies in the NSIDC database that are presented here. First, the geographical coordinates of the Baikal coastal stations in this database are inaccurate and have errors of several degrees. Assuming that the names of the stations are correct and the coordinates are not, we have corrected these errors to provide a new set of coordinates (Table 2) based on georeferenced GeoCover™ Landsat Thematic Mapper orthorectified mosaics with 28.5 m pixel size available from the MrSID Image Server (MrSID web site, 2003).

Table 2
Baikal coastal stations from the Lake and River Database at NSIDC, including corrected coordinates and the beginning and the end of available observations

Station name				
	Listvyanka	Baikal'sk	Nizhneangarsk	Bukhta
NSIDC metadata				
Name	Lake Baikal	Lake Baikal at Baikal'sk	Lake Baikal (N. Angarsk)	Lake Baikal (p. Bukhta)
Code	NG1	VSV1	VSV5	VSV8
Lon	105	107.5	104.25	109.47
Lat	51.66	53.5	52.8	53
Corrected coordinates				
Lon	104.87	104.17	109.56	105.43 [a]
Lat	51.85	51.53	55.77	52.15[a]
Data availability, years				
Start	1869	1983	1937	1931
End	1996	1987	1989	1989

[a] We give coordinates for Peschanaya bay.

The longest data series are available for the southern part of Lake Baikal (station NG1, apparently Listvyanka) from 1869 to 1996. About 50 years of data exist in the Northern Baikal (Nizhneangarsk) and at another station (p. Bukhta). The NSIDC coordinates for p. Bukhta are on land, and the data probably refer to the Peschanaya Bay on the northern shore of Southern Baikal facing the Selenga delta. For Baikal'sk, at the southern end of the lake, data are available for only 5 years. Only the data from Listvyanka cover the period of T/P and SSM/I observations.

Comparing LIN RAS and NSIDC data, we also have found small discrepancies in the ice formation dates and significant errors in the ice break-up dates since 1991. The NSIDC ice break-up dates are often 10–20 days later than the LIN RAS dates. We have informed Dr. Benson and NSIDC staff on these discrepancies, and they have commented that *"these discrepancies in ice out dates are due to a change in observers and criteria for ice out in the early 1990's. To be consistent with earlier records that used the beginning of ice break as the ice off date, we are correcting the data since 1991 in our database."* After these corrections were implemented, the dates for ice formation and break-up at Listvyanka are the same for the NSIDC and LIN RAS data sets (see Tables 4 and 5).

3. Ice cover discrimination algorithms

In order to discriminate ice from open water we use an algorithm that was developed for simultaneous active and passive microwave data from T/P altimetric data and passive microwave data from SMM/I (Kouraev et al., 2003, 2004a,b). Until now we have applied this ice/water discrimination approach only to the T/P data for various natural surfaces. This is the first time we apply it to a wide range of the existing satellite radar altimetry missions: T/P, TPNO, Jason-1, ENVISAT and GFO.

3.1. Simultaneous active and passive microwave data from satellite altimetry

As noted in Section 2.1, all existing satellite radar altimetry missions provide simultaneous nadir-looking active (radar altimeter) and passive (radiometer) microwave measurements from the same satellite platform. These measurements have been successfully used for studies of snow covered regions using data from the T/P and SSM/I satellites (Papa et al., 2002), and also for sea and lake ice cover parameters (Kouraev et al., 2003, 2004a,b).

The ice discrimination method was initially developed for the T/P data and is described in detail in (Kouraev et al., 2003, 2004). This method is based on the spatio-temporal evolution of the two T/P parameters. The first parameter is the backscatter coefficient at 13.6 GHz ($\sigma 0$), which is the ratio between the power reflected from the surface and the incident power emitted by the onboard radar altimeter, expressed in decibels (dB). The second parameter is the average value of the brightness temperature values at 18 and 37 GHz (Ulaby et al., 1986), measured in K, which we call TB2. Open water has a low backscatter coefficient and low brightness temperature values, while ice cover is characterised by a high backscatter coefficient and elevated brightness temperatures. When threshold values for backscatter and brightness temperatures are applied, we can distinguish between open water and ice with a high degree of reliability, compared with using either parameter on its own.

For many seasonally ice-covered seas and lakes (we have analysed the Caspian, Aral (Kouraev et al., 2003, 2004a,b), Azov, Baltic and White Seas, Hudson Bay (unpublished) and Onega and Baikal Lakes), the distribution of observations always reveals two distinctive clusters, representing open water and ice (Fig. 3a). Moreover, the temporal evolution of observations (Fig. 3b), suggests that during winter the radiometric properties of sea ice undergo further changes. Part of these changes can be attributed to the radar/radiometer footprint geometry and to ice floes distribution or ice edge location; this issue was addressed in detail in Kouraev et al. (2004). However, most of these changes are associated with variations in ice roughness, the development of snow cover, ice decay and other factors.

Ice formation results in a rapid progression of the radiometric properties (see Fig. 3) from point A (open water) to point B (young ice, with a high backscatter value due to its high reflectance and still relatively low brightness temperature). This transition is well observed in November and December. As the ice develops, the points shift from B to C (January–February). The point C is where the maximum number of ice cover observations occur. Snow accumulation, ice ageing and decay induce a further decrease in the backscatter values and changes in brightness temperature, resulting in the progression along the lines C–D and C–E (April–May). Ice break-up and melting (May–June) result in a rapid return to the point A (open water).

Observations from the four different satellite altimetry missions show a similar distribution (Fig. 4). Although the data from TPNO represent a different geographic region, they have a similar distribution to the original T/P observations, with a smaller number of absolute values due to the shorter mission duration.

The other missions (Jason-1, ENVISAT and GFO) have a similar distribution, again yielding two distinctive clusters corresponding to open water and ice/snow. However, the quality checking algorithms used by the data processing and distributing agencies apparently differ from that of T/P. For instance, for Lake Baikal there are no data with backscatter values higher than 33 dB for Jason-1 and higher than 31 dB for GFO. Moreover, for Jason-1 almost all the data acquired over the ice are filtered out in the initial Geophysical Data Records (GDRs), which reduces its temporal resolution especially for estimating the timing of ice formation and break-up. This is unfortunate, since Jason-1 has a very high radiometric resolution and along-track spatial resolution for the simultaneous active and passive microwave observations (Kouraev et al., 2003). In this study, we have used Jason-1 data to reliably detect open water. In the future, access to the unfiltered Jason-1 data could provide information for both ice and open water conditions.

3.2. Passive microwave data from SSM/I

Passive microwave data from SMMR and SSM/I sensors have been extensively used by the scientific community to estimate Arctic and Antarctic sea ice cover. The most commonly used algorithms for estimating ice cover concentration from passive microwave data, are the NASA Team and Bootstrap algorithms (Comiso, 1986; Steffen et al., 1992; Swift & Cavalieri, 1985). These algorithms use various combinations of brightness temperature (TB) data from the 19.35 (18.0 for SMMR) and 37.0 GHz horizontally (H) and vertically (V) polarised channels. The NASA Team algorithm uses the polarisation (PR) and spectral (GR) gradient ratios, defined by

$$\mathrm{PR} = \frac{\mathrm{TB19}V - \mathrm{TB19}H}{\mathrm{TB19}V + \mathrm{TB19}H} \quad (1)$$

$$\mathrm{GR} = \frac{\mathrm{TB37}V - \mathrm{TB19}H}{\mathrm{TB37}V + \mathrm{TB19}H}. \quad (2)$$

Further development of application of passive microwave data from SMMR and SSM/I has resulted in the improvement of the existing algorithms by adding other frequencies (such as 85 GHz) and by development of new algorithms (Belchansky et al., 2004; Kaleschke et al., 2001; Markus & Cavalieri, 2000; Svendsen et al., 1987).

However, ice discrimination using passive microwave techniques requires a good knowledge of the radiometric properties of the ice for each specific natural object. We have seen from altimetry that open water and ice form two well defined and easily separated clusters. However, for algorithms using passive microwave data alone the absence of in situ measurements of ice and water radiometric properties over the Lake Baikal is a problem for selecting tie-points. Also, although

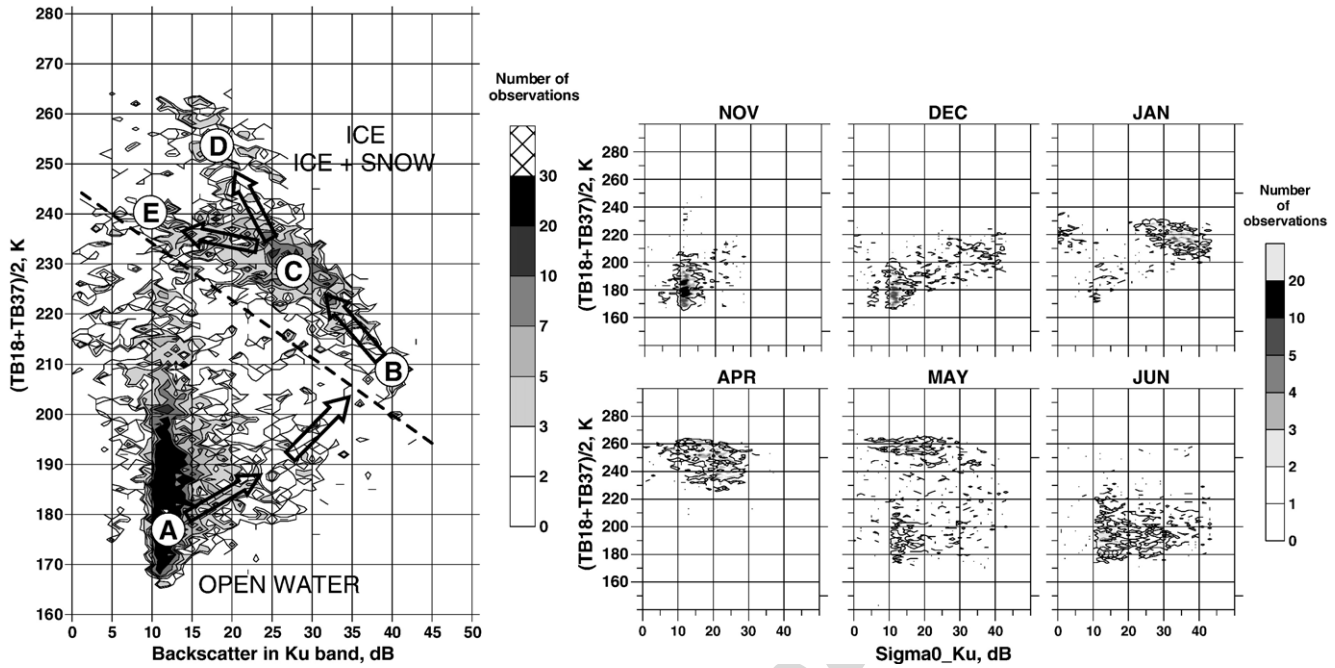

Fig. 3. Two-dimensional histograms (number of cases) for the whole year (left panel) and selected months (right panel) of T/P observations for Lake Baikal for 1992–2000. The axes show the backscatter coefficient in Ku band (13.6 GHz) versus the average value of brightness temperature at 18 and 37 GHz. Two main clusters (open water and ice/ice+snow) are shown on the left panel, as well as an the boundary between them (dashed line). Arrows show the temporal evolution of the various phases of ice formation, ageing, snow accumulation and melting.

the PR and GR parameters allow us to estimate both ice concentration and type for the Arctic and Antarctic sea ice (Steffen et al., 1992; Ulaby et al., 1986), for lake ice it is sometimes difficult to distinguish between ice and water (Fig. 5). Currently we apply a simplified algorithm that uses the PR and GR ratios with a threshold in order to distinguish between ice and open water (Fig. 5). The threshold is defined as a linear relationship between fixed PR and GR values for SSM/I.

Observations from SSM/I form two mixed clusters and ice discrimination becomes ambiguous. The closeness of the two clusters is apparently related to the radiometric properties of freshwater lake ice—our analysis for Ladoga lake (not presented here) shows a very similar distribution to the Lake Baikal observations in PR-GR space. Part of the problem may be due to land-to-water spillover effect (land contamination). This effect has been analysed in detail by Cavalieri et al. (1999) who implemented a land spillover correction algorithm, where a reduction coefficient for sea ice concentration (defined as a function of the closeness of the pixel to the shore) is introduced. However, the narrow and elongated shape of the Lake Baikal makes it difficult to select SSM/I pixels that are completely free of land. When we discard pixels with more than 30% land-coverage, we end up with 8 pixels for the Southern, 9 for the Middle and 15 for the Northern Baikal. Selecting only land-free pixels would result in only 1 pixel for the Southern, 4 for the Middle and 9 for the Northern Baikal, thus significantly reducing the coverage. Moreover, the brightness temperatures come from larger areas than the 25×25 km pixels, since the original spatial resolution is coarser (69×43 km for 19 GHz and 37×29 km at 37 GHz). In the following sections we keep all of the SSM/I data with less than 30% land-coverage for the joint altimetry-SSM/I analysis, although we are aware that some pixels may be contaminated by land influence. In case of doubt we consider that altimetry-derived ice cover parameters are of better quality than SMM/I data.

4. Ice discrimination methodology

The whole satellite data set has been processed using the ice discrimination methodology that consists of several steps. First, we use the two-dimensional histograms for the whole data set and for each satellite, to graphically define a set of thresholds values (shown as dashed lines on Figs. 4 and 5) which distinguish between open water and ice. These values are specific for each satellite and do not change with time. Then we convert these values to linear equations and apply them to the satellite data for each pentad. We then classify all processed altimetric and SSM/I data on the ice/water classification map for each pentad. Fig. 6 provides an illustration of a sequence of three such maps in May 2003, showing active ice decay processes. These maps show surface classification (open water or ice) from the four altimetric missions (Jason-1, TPNO, ENVISAT and GFO) overlaid on classification from the SSM/I sensor. To illustrate and validate our approach we complement this sequence with MODIS optical data (Fig. 7), available for this period (Irkutsk RICC website, 2005).

For pentad 27 (Fig. 6a) the whole Northern Baikal and most of the Middle Baikal are still ice-covered, as observed by both SSM/I and altimetry. Large areas of open water are observed for this pentad in the southern part of the Middle Baikal. Compared

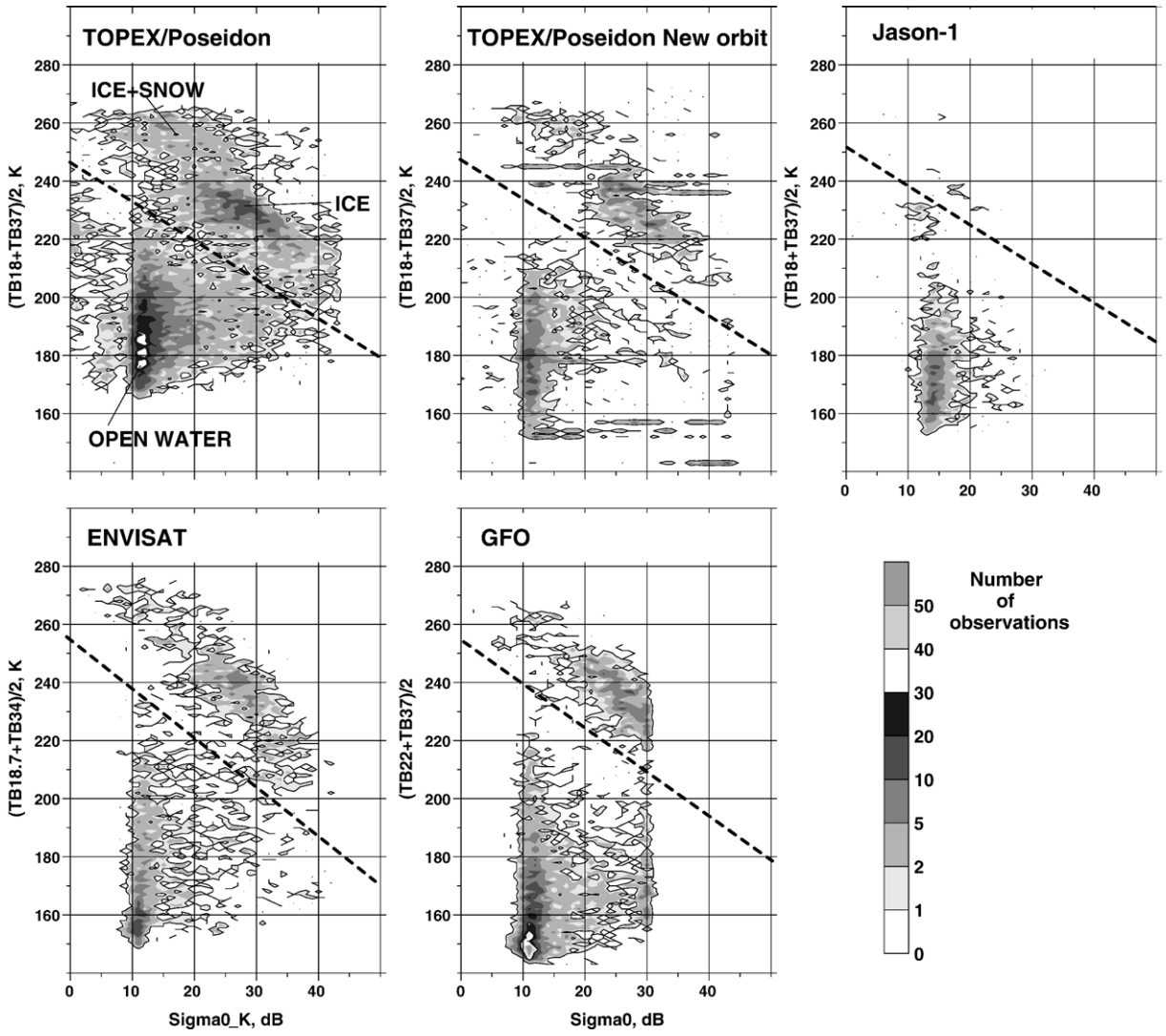

Fig. 4. Same as in Fig. 3, but for various altimetry missions. Note the differences in calculation of TB2 parameter (*Y*-axis) for ENVISAT and GFO that reflect changes in the available radiometer frequencies. Dashed lines represent the limits to separate open water and ice used in this study.

to SSM/I, the altimetric data are able to enhance the information content due to their high spatial resolution along the track. While the theoretical footprint of the altimeter data is about 12 km (see Section 2.1), the main part of the backscatter signal comes from a small area with a diameter of 1–2 km, which occur in the case of the quasi-specular signal over ice (Legrésy & Rémy, 1997). The high precision of ice edge detection using satellite altimeters has already been reported for the Caspian Sea using T/P data and MODIS imagery (Kouraev et al., 2003). One altimetric track (ENVISAT data for 15 May) shows the presence of open water near the Svyatoy Nos peninsula, which is not observed by SSM/I due its limited spatial resolution. The altimetric observations of open water correspond to a lead that appeared on the 12 May and then developed (Fig. 7a shows the MODIS image of this lead on 13 May). Some ice is still observed in the southern extremity of Lake Baikal by ENVISAT on 13 May (also confirmed by MODIS data on 13 May as floes of thin and broken ice, not shown here). Near the Selenga Delta, patches of thin drifting ice (visible on MODIS images for the 11 and 12 May, not shown here) have been observed on a TPNO track which crossed the lake on 11 May. They were not observed by another TPNO track along the lake on 12 May since they had moved southward.

During pentad 28 (Fig. 6b) the ice has retreated further north towards the Svyatoy Nos Peninsula, the location of the ice edge is well detected on the ENVISAT track from 20 May (Fig. 7b). Near the Selenga Delta we have one pixel classed as ice by SSM/I, but none of the three altimetric tracks confirmed this and we discard this pixel, as it is apparently contaminated by land.

For pentad 29 (Fig. 6c) almost all of the Middle Baikal is ice-free, except for the region near Ol'khon Island and some drifting ice floes near the eastern coast (detected both by MODIS and TPNO on 22 May, Fig. 7c). The TPNO detects ice when it is present at or near the nadir point within the altimeter footprint. This is why we have some discrepancy between the location of ice edge and ice-classed altimetric data for ice near Ol'khon Island and the drifting ice. The location of the ice edge on the boundary between the Middle and Northern Baikal,

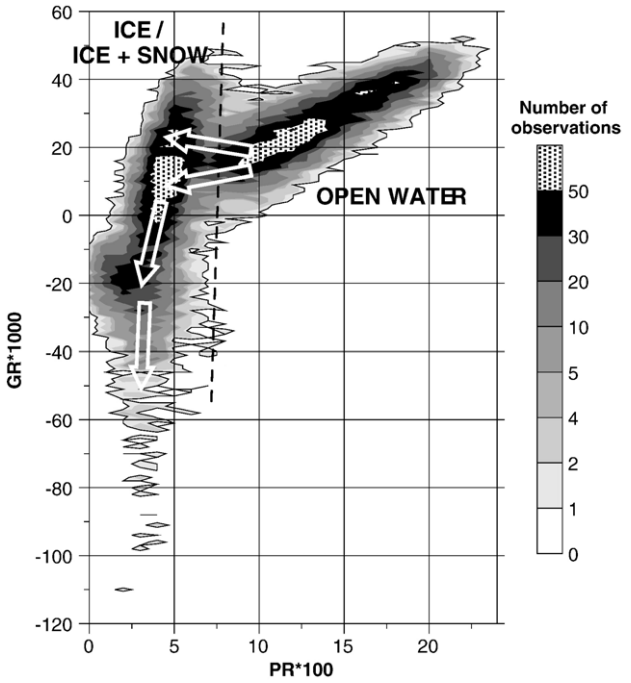

Fig. 5. Two-dimensional histograms (number of cases) for the whole year of SSM/I observations for Lake Baikal for 1992–2002 showing PR*100 versus GR*1000. Two main clusters (open water and ice/ice+snow) are shown, as well as the boundary between them (dashed line). Arrows show the temporal evolution of observations of ice formation, ageing, and snow accumulation.

perpendicular to the altimeter track, is well resolved by TPNO (Fig. 7c). While SSM/I shows one open water pixel for this area, we trust the altimetric data more and in this case we do not report the first open water SSM/I observation for the Northern Baikal for this pentad.

When the ice cover is well developed both approaches provide a robust discrimination between water and ice. However, for detecting young and rotten ice, these examples and our previous results (Kouraev et al., 2004c) show that the altimetric simultaneous active/passive data are more sensitive than the SSM/I passive data.

In order to assess the impact of altimetric data in improving ice/open water detection, we have compared ice event dates obtained using two data sets: (a) SSM/I and altimetric data and (b) SSM/I alone (Table 3). In many cases we did not find any difference. Altimetry brings no additional information when the whole lake is ice-covered, or in periods of rapid freezing or melting, when large lake areas undergo simultaneous changes (for example, melting in 1994/1995 and freezing in 1999/2000). However, for the Southern and Middle Baikal SSM/I sometimes provides first ice estimates that are too early, apparently related to signal contamination from land. In 1993 the first ice date was up to 25 days too early for Listvyanka and Middle Baikal, and 30 days too early for Southern Baikal (3 cases). In other cases, for Middle and Northern Baikal, SSM/I alone provides dates which are too late (5 to 15 days, 11 cases in total). In general, the dates for 100% ice cover are unambiguous using both data sets, except for Nizhneangarsk, when SSM/I alone gives later dates (5 to 10 days, in total 3 cases). Although the observation of the first water is also unambiguous (only one case of +5 days difference for Listvyanka and one case of +5 days for Nizhneangarsk), for 100% open water SSM/I alone sometimes gives dates that are either too early (5 days, 3 cases) or too late (3 cases, from +10 to +40 days). Once again, this is apparently related to land contamination. This inter-comparison shows that complementing SSM/I by altimetric observations improves the reliability of our estimates of ice events dates.

The two types of observations have specific advantages—wide spatial coverage and good temporal resolution for SSM/I and high radiometric sensitivity and along-track spatial resolution for altimetry. The combined altimetric-SSM/I observations significantly enhance the capabilities of microwave measurement for ice studies. During the analysis we have

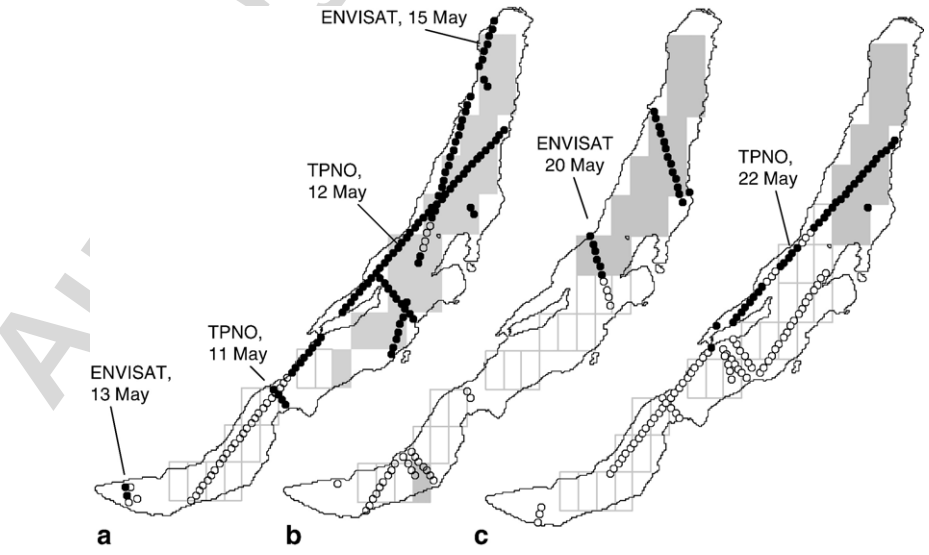

Fig. 6. A sequence of ice/water classification maps for May 2003. (a) pentad 27 (11–15 May), (b) pentad 28 (16–20 May), (c) pentad 29 (21–25 May). SSM/I classification: grey boxes—ice, white boxes—open water; altimetric data classification: black circles—ice, open circles—open water (no distinction is made between various altimeter missions). Altimetric tracks, discussed in the text, are marked.

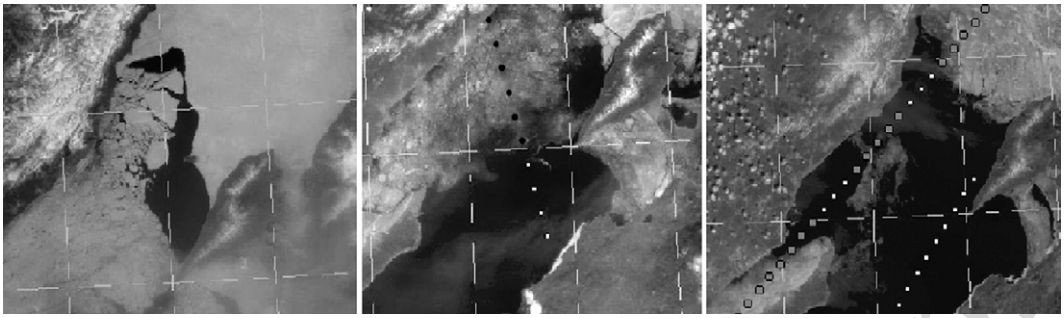

Fig. 7. Ice cover distribution in May 2003 from MODIS imagery (Irkutsk RICC website, 2005) and altimetric classification. (a) MODIS image for 13 May; (b) MODIS image for 19 May and ENVISAT classification for 20 May (ice—black circles, open water—white circles). (c) MODIS data for 22 May and ice classification (ice—large grey circles, open water—white circles) from TPNO (northern track, 22 May) and GFO (southern track, 23 May).

tried to ensure that both types of data agree with each other; in case of doubt, we gave priority to the altimetric data. Analysis of several consecutive maps usually significantly improves the reliability of the estimates. In some cases the SSM/I pixels near the coast were subject to potential land contamination such as when ice was observed for one pentad but not observed for the previous or later pentad. If there were no altimetric data to confirm this, we discarded these observations as unreliable.

It should be noted that the temporal resolution of altimetry data for large sub-basins, which are covered by several altimetric tracks, is significantly higher than the nominal repeat period. For example, the longer repeat period of ENVISAT and GFO is compensated by the density of satellite tracks over the Baikal. The information content from altimetry depends on the shape of the lake—one long track along the lake has probably as much information as two or three short tracks across. Fig. 8 shows the cumulative probability of altimetric coverage (expressed as length of tracks in km) over the whole Baikal for T/P (Jason-1 has the same orbit), ENVISAT and GFO. We do not take here into account TPNO—though its orbit is very good for Lake Baikal studies, the probability of having satellites on this orbit in the future is uncertain. We see that for a given pentad at the scale of the whole lake there is always at least one track that covers the lake. In the best case we have 220 km of satellite tracks for TP, 360 km for ENVISAT and 380 for GFO. The combination of two satellites significantly increases the spatial coverage for a given pentad (Fig. 8d–f), with TP+ENVISAT and TP+GFO providing similar coverage, and GFO+ENVISAT providing even denser spatial resolution. Combining three satellites (T/P+ENVISAT+GFO, Fig. 8g) further improves the coverage, with a minimal length of 160 km and a maximal one of 660 km. We are currently lucky enough to have all three satellites operating simultaneously, in the future this combination is not assured. Nevertheless, even one altimetric satellite in combination with SSM/I provides an important contribution to lake ice monitoring. As a result, the pentad-based classification maps always contain SSM/I data and a varying, but significant number of altimetric observations. We can define ice event dates using these maps with a five-day temporal resolution and an uncertainty of ±2.5 days.

5. Results

We have analysed classification maps for each pentad and have defined the dates corresponding to the various ice cover events. We have divided the lake onto three sections and two

Table 3
Difference in ice event dates between the two data sets (SSM/I only compared to SSM/I and altimetric data), in pentads (5 days)

	First ice					100% ice[a]	First open water[b]		100% open water				
Winter	L	SB	MB	NB	NA	NA	L	NA	L	SB	MB	NB	NA
1992/1993						+1							
1993/1994	−5/0	−6/−2	−4					−1		+8			
1994/1995				+1	+1								
1995/1996				+1	+1	+2							
1996/1997													
1997/1998		+1				+1							
1998/1999					+1/+3								
1999/2000												−1	−1
2000/2001			+1										+5
2001/2002			+2	+2	+2		+1		+2				
2002/2003			+1								−1		

Empty cells—no difference (0 days). L—Listvyanka, SB—Southern Baikal, MB—Middle Baikal, NB—Northern Baikal, NA—Nizhneangarsk.
[a] For 100% ice, the difference was found only for Nizhneangarsk.
[b] For first open water, the difference was found only for Listvyanka and Nizhneangarsk.

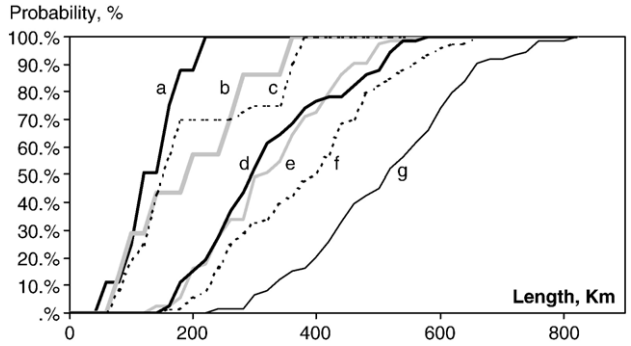

Fig. 8. Cumulative probability (in %) of altimetric track coverage (expressed as the total length of tracks, in km) over the whole Lake Baikal for orbits such as TP (the same orbit for Jason-1), ENVISAT (same orbit as ERS-1 and -2) and GFO. (a) T/P alone, (b) ENVISAT alone, (c) GFO alone, (d) T/P+GFO, (e) TP+ENVISAT, (f) GFO+ENVISAT, (g) T/P+ENVISAT+GFO.

sub-regions: Listvyanka, covered by the two leftmost SSM/I pixels in the south and the corresponding altimetric tracks, and Nizhneangarsk, covered by the two northernmost SSM/I pixels and the corresponding altimetric tracks. For each region we have defined four dates: the first appearance of ice, the formation of stable ice cover, the first appearance of open water and the complete disappearance of ice (Tables 4 and 5). In some cases the definition of ice event dates was uncertain due to: (a) data gaps for SSM/I or altimetric observations, (b) ambiguous ice detection related to land contamination of the microwave signal, and (c) consecutive freezing and melting events. In order to account for this uncertainty for each event we provide a time span of earliest and latest possible dates (Tables 4 and 5).

We have compared the in situ observations from LIN RAS with the satellite-derived estimates of the timing of ice events for the Listvyanka sub-region and for the Southern Baikal (Figs. 9–11). The LIN RAS date for ice formation is defined as the date when the whole area visible from the observation point at Listvyanka (usually 10–15 km) is completely covered with stable ice cover that stays until spring. The ice break-up date is defined as the date when the ice cover is broken and no longer observed in the observation area, though some ice fields can still be observed. The 100% ice-free dates are defined when ice and ice fields are no longer observed. Often the area visible from Listvyanka is reduced due to the presence of fog either over the lake area or by fog coming from the Angara valley to the lake. Therefore, in order to account for differences in the observation size, we compare Listvyanka data of ice formation with satellite-derived dates when 100% ice cover was observed, and for ice break-up—when the first open water was observed. The comparison of ice conditions in a relatively small area visible from the coastal station and large sub-region such as Listvyanka or the whole Southern Baikal is not straightforward and one should expect discrepancies.

For the freeze-up dates (Fig. 9), both the satellite estimates for Listvyanka and Southern Baikal show remarkably good agreement with the in situ data. After the winter of 1994/95 there is a marked tendency for ice to form earlier. In general satellites define ice formation slightly earlier, the differences are in the range of 2–6 days except for winter 2002/03 when the difference is 17 days. This delay can be explained by the differences in the observation area, and the specific ice formation and development character in December 2002–January 2003. According to the MODIS images (not shown here), at the end of December 2002 the whole central part of the Southern Baikal was already covered by ice fields, but the region near Listvyanka and the southern tip of Southern Baikal were still ice-free. After 5 January 2003 ice was well developed everywhere, except the central part of the Southern Baikal from Listvyanka to the Selenga delta, where ice was present but not continuous. Between 13–15 and 23–25 January 2003 this central part

Table 4
Ice formation from historical data (LIN RAS, Listvyanka) and satellite observations

			First ice observed					100% ice observed				
Winter	LIN RAS	NSIDC (old)	L	SB	MB	NB	NA	L	SB	MB	NB	NA
1990/1991	25	25										
1991/1992	3	3										
1992/1993	15	15	6/10	6/15	6/10	−19/−5	−19/−5	11/15	11/15	11/15	11/15	−9/−5
1993/1994	17	17	11/15	1/5	−4/10	−39/−25	−39/−25	11/15	11/15	16/30	11/15	−29/−25
1994/1995	35	28	−4/0	−4/0	n.a./15	−14/0	−14/0	26/30	26/30	26/30	26/30	−4/0
1995/1996	18	18	11/15	6/10	6/15	−4/0	−4/0	11/15	16/20	21/25	16/20	−4/0
1996/1997	22		1/20	−4/0	−9/−5	−19/−15	−19/−15	11/20	16/25	6/15	−4/0	−14/−10
1997/1998	12		6/10	−4/5	6/10	−9/0	−9/0	6/10	6/10	11/15	6/15	−4/0
1998/1999	19		6/10	1/10	6/10	−19/−15	−19/−15	11/15	11/15	6/10	6/10	−4/5
1999/2000	12		6/10	6/10	6/10	6/10	−4/5	6/10	6/10	6/10	6/10	6/10
2000/2001	5		−4/0	−9/−5	−9/−5	−24/−20	−24/−20	1/5	1/5	−9/−5	−9/−5	−24/−20
2001/2002	24		16/20	6/10	6/10	−14/−10	−14/−10	16/20	21/25	21/25	21/25	1/5
2002/2003	15(25)[a]		−4/0	−14/−10	−4/0	−19/−15	−19/−15	−4/0	−4/0	−4/0	−4/0	−19/−15
2003/2004	27		6/15	6/15	6/15	−4/15	−4/15	16/25	11/20	11/20	11/20	11/20

All data are in days from 31 December. LIN RAS data show dates of 100% ice cover. We also provide the old uncorrected values ("NSIDC old"). Satellite-derived data show the dates of first appearance of ice and 100% of ice cover. For satellite-derived data both the earliest and latest possible dates are provided ("early/late"). L—Listvyanka, SB—Southern Baikal, MB—Middle Baikal, NB—Northern Baikal, NA—Nizhneangarsk.

[a] The first date (15) is more reliable as it shows ice conditions in the Listvennichniy bay. The second date (25) is based on observation of fog over small area outside of the bay, but it is not clear whether the fog has been observed over small polynyas or over thin young ice.

Table 5
Same as Table 4, but for ice break-up

	LIN RAS		NSIDC old	First open water observed					100% open water observed				
Winter	Ice break-up	100% ice-free		L	SB	MB	NB	NA	L	SB	MB	NB	NA
1990/1991	117	128	117										
1991/1992	137	140	140	136/140	136/140	136/140	146/150	146/150	136/140	141/155	141/145	151/155	151/155
1992/1993	112	127	127	131/140	121/130	121/130	131/135	136/145	141/145	126/140	141/145	141/150	141/150
1993/1994	118	126	126	131/135	121/130	131/135	136/145	156/160	131/135	131/140	146/160	156/160	156/160
1994/1995	113	123	123	126/130	126/130	131/135	136/140	146/150	131/135	131/140	136/140	151/155	151/155
1995/1996	121	130	130	131/135	126/130	126/130	136/140	146/150	131/135	131/140	131/140	151/155	151/155
1996/1997	117	121		116/120	116/120	121/130	141/145	141/145	121/125	126/135	136/145	141/145	141/145
1997/1998	119	128		131/135	121/130	121/125	141/145	146/150	131/135	136/140	136/140	146/150	146/150
1998/1999	121	130		121/130	121/130	126/130	146/150	156/160	126/130	126/130	141/145	156/160	156/160
1999/2000	119	126		126/130	126/130	126/130	141/145	141/145	126/130	126/130	136/140	146/150	146/150
2000/2001	132	143		146/150	141/145	146/150	156/160	161/165	146/150	146/150	151/155	161/165	161/165
2001/2002	109	131		131/135	111/115	126/130	126/130	151/155	136/140	136/140	136/140	161/165	181/200
2002/2003	120	127		126/130	126/130	131/135	146/150	151/155	126/130	126/150	146/150	156/160	156/160
2003/2004	122	135		131/135	n.a.	121/130	146/150	n.a.	131/135	131/135	131/140	161/165	n.a.

For LIN RAS we provide two estimates—dates of ice break-up and of 100% ice-free observations. NSIDC recently corrected data now use LIN RAS data for ice break-up. Satellite-derived data show dates of first appearance of open water and 100% of open water.

became ice covered, but cracks and polynyas were still observed in winter. Apparently, during this time the formation of a stable ice cover was disrupted by the wind. It is known that ice formation in Listvyanka occurs later than in other regions of the Southern Baikal, due to the influence of the strong north-western winds coming from the Angara River valley.

Concerning the ice break-up dates (Fig. 10), the satellite estimates of first open water observed were later than the Listvyanka data estimates of ice break-up, but surprisingly were in better agreement with the 100% open water dates from the Listvyanka data (difference of 1–2 days, rarely 7–8 days). This is related to the definition of the end of the ice seasons at the coastal stations, and to the difference between the size of the region observed from the coast and the much larger lake area observed by satellite. Both the LIN RAS and satellite data show a tendency towards a later ice break-up in the 1990s.

Satellite data provide a good observation of the interannual dynamics of ice break-up at the scale of the sub-basin, while observations at a specific coastal station could be biased. While ice formation is mainly determined by thermal influence ice break-up is more affected by dynamical factors (Kouraev et al., in press). The differences between the satellite data and data from Listvyanka (or any other specific observation point) could be explained by specific local conditions in each specific year (wind drift of ice floes, influence of wind on ice break-up, etc.). After the ice cover has disappeared near the coast, where the wind and temperature influence is more pronounced, it may still be observed offshore in the central part of the lake. This explains why the satellite-derived ice break-up dates are later, compared to the observations at the coast. In this respect, the satellite observations are more representative of ice break-up for large regions of the lake, rather than data from specific coastal stations.

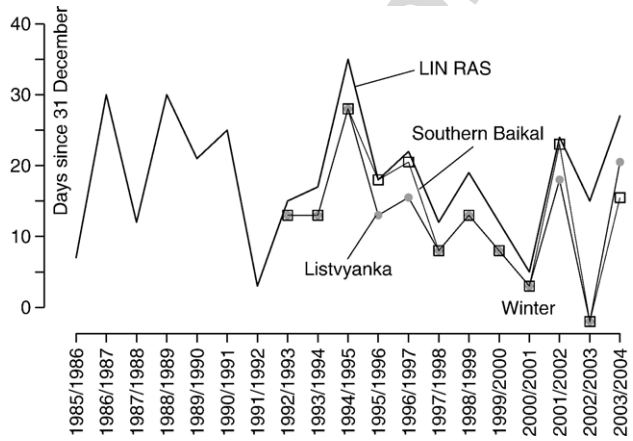

Fig. 9. Freeze-up dates from historical (thick black line, LIN RAS data) and satellite-derived data (average values) for 100% ice coverage (black line with grey dots—Listvyanka, black line with open rectangles—whole Southern Baikal).

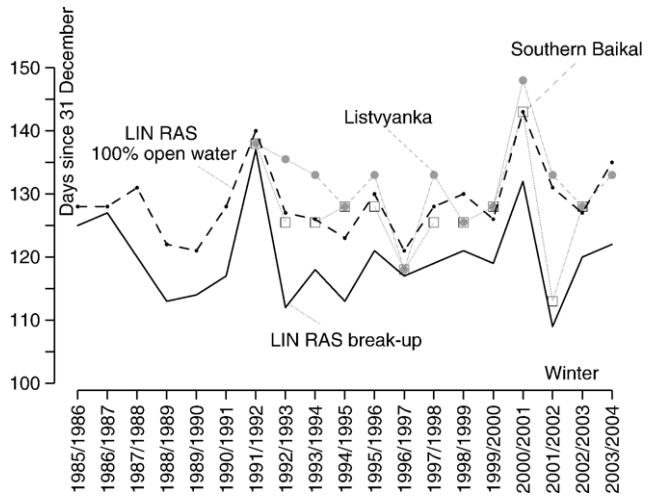

Fig. 10. Break-up date from historical (LIN RAS data, thick black line—ice break-up, dashed line with black circles—100% open water) and satellite-derived data (average values) for first open water observation (black line with grey dots—Listvyanka, black line with hollow rectangles—whole Southern Baikal).

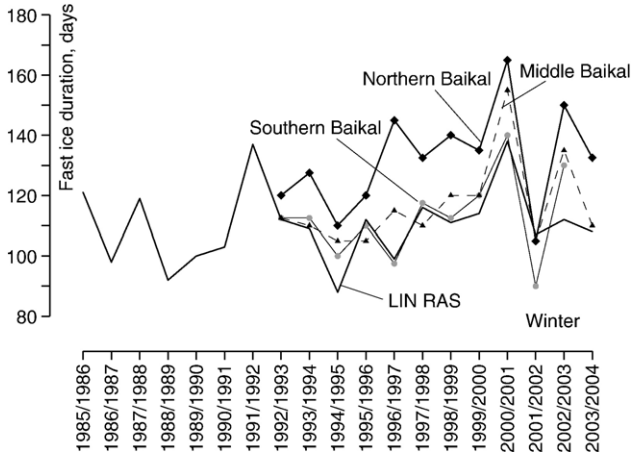

Fig. 11. Fast ice duration from historical (LIN RAS data, thick black line, calculated as difference between 100% open water and ice formation date) and satellite-derived data (average difference in timing between 100% ice cover observation and appearance of first open water). Line with grey dots—Southern Baikal, dashed line with black triangles—Middle Baikal, thick line with black diamonds—Northern Baikal.

Moreover, the analysis of ice event dates (not shown here) for Listvyanka and other coastal stations since 1951 (date of the beginning of observations on most coastal stations) shows that ice break-up conditions in the Listvennichniy bay, where the Listvyanka station is located, differ from that for other stations. While many coastal stations are protected by mountains, at Listvyanka station the north-western winds can penetrate through the large valley of the Angara River. As a result, ice break-up for Listvyanka station is observed earlier, and interannual changes of break-up dates differ from observations at other stations. It is worthwhile to note that this difference is not observed for ice formation dates, since during this period the intrusion of cold air masses brings strong winds and the dynamic influence is more or less homogeneous over the whole region.

Fast ice duration also shows very good agreement between the historical data and satellite-derived estimates (Fig. 11), with differences less than 5 days, except for 1994–1995 and 2002–2004. The interannual variability of the fast ice duration is similar for the three parts of Lake Baikal. Northern Baikal has the longest fast ice duration, while the duration in the Middle and Southern Baikal alternates. The main factor explaining the differences in ice development in the different regions of Lake Baikal is climate. Due to the latitudinal extent of the lake, the air temperature over the lake changes significantly from South to North. According to Verbolov et al. (1965), the 1896–1959 average annual air temperature for the Southern, Middle and Northern Baikal was −1.3, −1.9 and −3.2 °C, respectively, and average temperature for the cold period (December–May) was −9.3, −10.0 and −11.7 °C, respectively. Earlier ice formation and later ice break-up in the Northern Baikal are also related to relatively weak wind speed. During ice formation in December–January, the Southern and Middle Baikal average wind speed is 4.5–4.7 m/s, while in the Northern Baikal it is 3.2 m/s. During ice break-up these values are 3.8–3.9 m/s for the Southern and Middle Baikal, and 2.6 m/s for the Northern Baikal (Verbolov et al., 1965). Thus weaker winds are partly responsible for the later ice-break-up in Northern Baikal.

The cross-comparison of historical and satellite-derived series shown in this section shows that the Lake Baikal ice phenology derived from a combination of active and passive microwave observations from radar altimetric missions and SSM/I can be reliably used to extend the existing time series available for coastal stations, and also to create new time series for different parts of Baikal which were not previously covered by continuous in-situ observations.

6. Discussions and conclusions

A comparison between historical in situ data and a combination of altimetric and radiometric observations shows the significant potential of satellite observations for the study of ice cover on lakes. We have proposed lake ice discrimination algorithms and a methodology based on the combined use of the data from the four altimetric missions and SSM/I. Validation of the satellite-derived classification using available in situ observations and visible imagery from MODIS shows the reliability of our approach and the high sensitivity of altimetric data for detecting thin and broken ice, leads and ice edges. We have applied this approach to the entire satellite data set and have defined specific dates for ice formation, including the first appearance of ice, the formation of stable ice cover, the first appearance of open water, and the complete disappearance of ice and their associated uncertainties. Using these satellite-derived estimates we have reliably extended the existing time series of ice events up to 2004 in the Southern Baikal, and provided new information on the Middle and Northern Baikal, where no recent in-situ ice cover observations are available.

From 1992–2004, the satellite-derived data reliably reproduce the interannual dynamics of the ice regime recorded at the coastal stations. We obtain a better relation for ice formation dates than for ice break-up dates, since during spring influence of local factors is more pronounced and this brings heterogeneity to the in-situ observations. Lake Baikal has a large surface area and complex hydrological and wind regimes in its various sub-regions. So satellite observations provide important additional information on the ice regimes and their interannual variability, since they provide an assessment of the ice regime over large parts of the lake surface that are not sampled with coastal station measurements. Our data show that over the last 10–15 years, there is a tendency for longer fast ice duration over the whole Lake Baikal due to a tendency for earlier ice formation and later ice break-up.

If we consider the long-term series of fast-ice duration since 1868 (Fig. 12) we observe high frequency variability superimposed on longer-term changes. There was a marked decrease in fast ice duration from 1868 up to the 1930s, then this tendency slowed and has been oscillating. Over the short period from 1992–2004, we observe high interannual variability and an increase in the fast ice duration. This recent tendency for longer ice duration is in agreement with the long-period cycles of the Baikal ice regime. In the 20th century several sub-century cycles (20–30 years long) have been identified for air

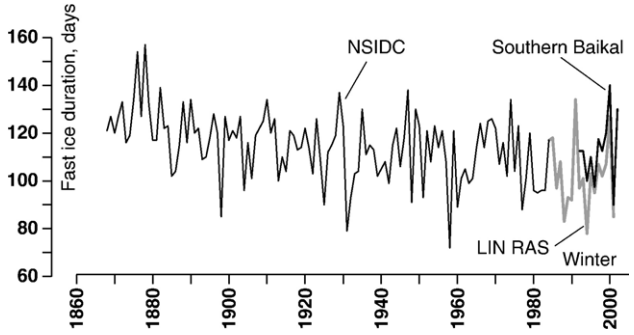

Fig. 12. Long-term fast ice duration from historical and satellite data. Thin black line—NSIDC data (up to 1984), thick grey line—LIN RAS data, thick black line—Southern Baikal (calculated as for Fig. 8).

temperature series in the Lake Baikal region (Shimaraev et al., 2002a,b). One of these cycles started in the 1970s and is characterised by warmer air temperature during the 1990s and cooling afterwards.

Ice conditions over the last decades are characterised by high interannual variability and this reflects the complexity of the underlying physical processes. It also stresses the need for long, continuous and homogeneous time series of ice parameters to assess recent trends. In this respect, changes made to the Lake and River Ice Phenology Database at the NSIDC (see Section 2.2.1) are very important.

The lake ice discrimination approach based on combination of altimetry and radiometry data has been tested for Lake Baikal, but could be easily applied to other lakes and water bodies with seasonal ice cover. Future developments will include an extensive validation of the algorithms using in situ and other types of satellite data, as well as an assessment of the possibility of estimate snow depth over ice using the active and passive microwave observations. Another promising aspect will be to explore the dual-frequency capabilities of T/P and ENVISAT radar altimeters. We also plan to correlate our new data on Lake Baikal ice conditions with indices of global climate variability to improve our understanding of the natural processes in the Baikal region and their teleconnections.

Analysis of the temporal and spatial ice coverage of Lake Baikal from several altimetric missions and SSM/I shows that the combination of wide spatial coverage and temporal resolution of SSM/I and high radiometric sensitivity and along-track spatial resolution of altimetric satellites significantly enhances the capabilities of microwave measurement for ice studies. Finally, for large sub-basins, the use of several altimetric missions increases not only the spatial, but also the temporal coverage, providing information on large-scale changes more frequently than the nominal repeat period for any individual satellite. As a result, the pentad-based classification maps always contain SSM/I data and a varying, but significant number of altimetric observations. Future satellite missions, such as Jason-2 or a constellation of small altimetric satellites such as AltiKa, as well as missions with interferometric radar altimeters, such as Cryosat-2 and the proposed hydrology-dedicated mission WatER, will further advance spatial and temporal coverage of the Earth surface and improve our understanding of various natural phenomena, including ice regime of continental water bodies.

Acknowledgments

We would like to dedicate this article to our friend and colleague, Sergei Valeryevich Semovski, who sadly passed away on the 2nd of June 2006. Sergei was an initiator of this work on the Lake Baikal ice cover. We miss him very much.

We are grateful for the Center for Topographic studies of the Oceans and Hydrosphere (CTOH) at LEGOS, Toulouse, France for provision of the altimetric data. We thank Martin Schmid (Eawag, Kastanienbaum, Switzerland) for help with obtaining historical ice timing data and his constructive remarks for the manuscript. We also thank Martin Todd and Anson Mackay (both from the Department of Geography, University College London, United Kingdom), as well as anonymous reviewers, for their helpful comments on the manuscript. We are also grateful to Rosemary Morrow (LEGOS, Toulouse, France) for her help with the manuscript revision. The research has been partly supported by the AICSEX (Arctic Ice Cover Simulation Experiment) Project of the 5th framework program of the European Commission and RFBR (Russian Foundation for Basic Research) Grant No. 04-05-64839.

References

Armstrong, R. L., Knowles, K. W., Brodzik, M. J., & Hardman, M. A. (2003). *DMSP SSM/I Pathfinder daily EASE-Grid brightness temperatures.* Boulder, CO: National Snow and Ice Data Center Digital media and CD-ROM.

Atlas of the Lake Baikal. (1993). *Russian Academy of Sciences, Siberian branch.* Moscow: Federal Service of geodesy and cartography 160 pp. (In Russian).

Belchansky, G. I., & Douglas, D. C. (2000). Classification methods for monitoring Arctic sea ice using Okean passive/active two-channel microwave data. *Journal of Remote Sensing and Environment*, *73*, 307−322.

Belchansky, G. I., & Douglas, D. C. (2002). Seasonal comparisons of sea ice concentration estimates derived from SSM/I, OKEAN, and RADARSAT data. *Journal of Remote Sensing and Environment*, *81*, 67−81.

Belchansky, G. I., Douglas, D. C., Alpatsky, I. V., & Platonov, N. G. (2004). Spatial and temporal multiyear sea ice distributions in the Arctic: A neural network analysis of SSM/I data, 1988–2001. *Journal of Geophysical Research*, *109*, C10017. doi:10.1029/2004JC002388

Benson, B., & Magnuson, J. (2000). *Global lake and river ice phenology database.*Boulder, CO: National Snow and Ice Data Center/World Data Center for Glaciology, Boulder. Digital media.

Burns, B. A., Cavalieri, D. J., Keller, M. R., Campbell, W. J., Grenfell, T. C., Maykut, G. A., et al. (1987). Multisensor comparison of ice concentration estimates in the marginal ice zone. *Journal of Geophysical Research*, *92* (C7), 6843−6856.

Cavalieri, D. J., Burns, B. A., & Onstott, R. G. (1990). Investigation of the effects of summer melt on the calculation of sea ice concentration using active and passive microwave data. *Journal of Geophysical Research*, *95* (C4), 5359−5369.

Cavalieri, D. J., Parkinson, C. L., Gloersen, P., Comiso, J. C., & Zwally, H. J. (1999). Deriving long-term time series of sea ice cover from satellite passive-microwave multisensor data sets. *Journal of Geophysical Research*, *104*(C7), 15803−15814.

Comiso, J. C. (1986). Characteristics of Arctic winter sea ice from satellite multispectral microwave observations. *Journal of Geophysical Research*, *91*, 975−994.

Emery, W. J., Fowler, C., & Maslanik, J. (1994). Arctic sea ice concentrations from special sensor microwave imager and advanced very high

resolution radiometer satellite data. *Journal of Geophysical Research*, *99*, 18329−18342.

Galaziy, G. I. (1987). *Baikal in questions and answers.*Irkutsk: Eastern-Siberian publishing (In Russian).

Granin, N. G., Jewson, D. H., Grachev, M. A., Levin, L. A., Zhdanov, A. A., Averin, et al. (1999). Turbulent mixing in the water layer just below the ice and its role in development of diatomic algae in Lake Baikal. *Doklady Akademii Nauk*, *366*, 835−839.

Irkutsk RICC website (2005). http://geol.irk.ru/bricc.htm

Kaleschke, L., Lupkes, C., Vihma, T., Haarpaintner, J., Bochert, A., Hartmann, J., et al. (2001). SSM/I sea ice remote sensing for mesoscale ocean–atmosphere interaction analysis. *Canadian Journal of Remote Sensing*, *27*(5), 526−537.

Kouraev, A. V., Papa, F., Buharizin, P. I., Cazenave, A., Crétaux, J. -F., Dozortseva, J., et al. (2003). Ice cover variability in the Caspian and Aral seas from active and passive satellite microwave data. *Polar Research*, *22* (1), 43−50.

Kouraev, A. V., Papa, F., Mognard, N. M., Buharizin, P. I., Cazenave, A., Crétaux, J. -F., et al. (2004a). Sea ice cover in the Caspian and Aral seas from historical and satellite data. *Journal of Marine Systems*, *47*, 89−100.

Kouraev, A. V., Papa, F., Mognard, N. M., Buharizin, P. I., Cazenave, A., Crétaux, J. -F., et al. (2004b). Synergy of active and passive satellite microwave data for the study of first-year sea ice in the Caspian and Aral seas. *IEEE Transactions on Geoscience and Remote Sensing (TGARS)*, *42* (10), 2170−2176.

Kouraev, A. V., Semovski, S. V., & Mognard, N. M. (2004). Ice cover of the Baikal lake: Historical and satellite measurements. *Geophysical Research Abstracts, EGU General assembly*, *Vol. 6*. 00565, SRef-ID: 1607-7962/gra/EGU04-A-00565. European Geosciences Union, CD-ROM.

Kouraev, A. V., Semovski, S. V., Shimaraev, M. N., Mognard, N. M., Légresy, B., & Remy, F. (in press). Ice regime of Lake Baikal from historical and satellite data: Influence of thermal and dynamic factors. *Limnology and Oceanography* under revision, manuscript no L&O-06-012.

Legrésy, B., & Rémy, F. (1997). Altimetric observations of surface characteristics of the Antarctic ice sheet. *Journal of Glaciology*, *43*(144), 265−275.

Livingstone, D. (1999). Ice break-up on southern Lake Baikal and its relationship to local and regional air temperatures in Siberia and the North Atlantic Oscillation. *Limnology and Oceanography*, *44*, 1486−1497.

Mackay, A. W., Battarbee, R. W., Flower, R. J., Granin, N. G., Jewson, D. H., Ryves, D. B., et al. (2003). Assessing the potential for developing internal diatom-based inference models in Lake Baikal. *Limnology and Oceanography*, *48*, 1183−1192.

Mackay, A. W., Ryves, D. B., Battarbee, R. W., Flower, R. J., Jewson, D., Rioual, P., et al. (2005). 1000 years of climate variability in central Asia: Assessing the evidence using Lake Baikal diatom assemblages and the application of a diatom-inferred model of snow thickness. *Global and Planetary Change*, *46*, 281−297.

Magnuson, J. J., Robertson, D. M., Benson, B. J., Wynne, R. H., Livingstone, D. M., Arai, T., et al. (2000). Historical trends in lake and river ice cover in the northern hemisphere. *Science*, *289*(5485), 1743−1746.

Markus, T., & Cavalieri, D. J. (2000). An enhancement of the NASA Team sea ice algorithm. *IEEE Transactions on Geophysical and Remote Sensing*, *38* (3), 1387−1398.

MrSID Image server. (accessed 2003). NASA. https://zulu.ssc.nasa.gov/mrsid/mrsid.pl

Papa, F., Legresy, B., Mognard, N., Josberger, E. G., & Remy, F. (2002). Estimating terrestrial snow depth with the TOPEX/Poseidon altimeter and radiometer. *IEEE Transactions on Geoscience Remote Sensing*, *40*, 2162−2169.

Semovski, S. V., & Mogilev, N. Yu. (2003). Ice and snow cover of Lake Baikal—application of satellite imagery in investigating their dynamics. *Nordic Hydrology*, *34*, 33−50.

Semovski, S. V., Mogilev, N. Yu., & Sherstyankin, P. P. (2000). Lake Baikal ice: Analysis of AVHRR imagery and simulation of under-ice phytoplankton bloom. *Journal of Marine Systems*, *27*, 117−130.

Shimaraev, M. N., Domysheva, V. M., Sinyukovich, V. N., Kuimova, L. N., & Troitskaya, E. S. (2003). Manifestation of global climatic changes in Lake Baikal during the 20th century. *Proceedings of the 7th workshop on physical processes in natural waters 2–5 July 2003. Petrozavodsk, Russia* (pp. 161−164). Petrozavodsk.

Shimaraev, M. N., Kuimova, L. N., Sinyukovich, V. N., & Tsekhanovskii, V. V. (2002a). Manifestation of global climatic changes in Lake Baikal during the 20th century. *Doklady Earth Sciences*, *383A*, 288−291.

Shimaraev, M. N., Kuimova, L. N., Sinyukovich, V. N., & Tsekhanovskii, V. V. (2002b). Climate and hydrological processes in the basin of Lake Baikal in the XXth century. *Meteorology and Hydrology*, *3*, 71−78 (in Russian).

Steffen, K., Key, J., Cavalieri, D. J., Comiso, J., Gloersen, P., St.Germain, K., et al. (1992). The estimation of geophysical parameters using passive microwave algorithms. In F. D. Carsey (Ed.), *Microwave remote sensing of sea ice AGU: Geophysical Monograph*, *Vol. 68*.

Svendsen, E., Mätzler, C., & Grenfell, T. C. (1987). A model for retrieving total sea ice concentration from spaceborne dual-polarised passive microwave instrument operating near 90 GHz. *International Journal of Remote Sensing*, *8*(10), 1479−1487.

Swift, C. T., & Cavalieri, D. J. (1985). Passive microwave remote sensing for sea ice research. *EOS*, *66*(49), 1210−1212.

The INTAS Project 99-1669 Team (2002). A new bathymetric map of Lake Baikal. *Open-File Report on CD-ROM*.

Todd, M. C., & Mackay, A. W. (2003). Large-scale climatic controls on Lake Baikal ice cover. *Journal of Climate Volume*, *16*(19), 3186−3199.

Ulaby, F. T., Moore, R. K., & Fung, A. K. (1986). *Microwave remote sensing, active and passive. From theory to applications*, *Vol. III*. Artech house, Inc.

Verbolov, V. I., Sokol'nikov, V. M., & Shimaraev, M. N. (1965). *Hydrometeorological regime and heat balance of the Lake Baikal.* Moscow-Leningrad: "Nauka" publishers 373 pp. (In Russian).

Wüest, A., Ravens, T. M., Granin, N. G., Kocsis, O., Schurter, M., & Sturm, M. (2005). Cold intrusions in Lake Baikal: Direct observational evidence for deep-water renewal. *Limnology and Oceanography*, *50*(1), 184−196.